

Conjugated Oligothiophene-Dendron-Capped CdSe Nanoparticles: Synthesis and Energy Transfer

Jason Locklin, Derek Patton, Suxiang Deng, Akira Baba, Mitchel Millan, and Rigoberto C. Advincula*

Department of Chemistry, University of Houston, Houston, Texas 77204

Received June 29, 2004. Revised Manuscript Received September 3, 2004

In this study, we demonstrate the synthesis of branched oligothiophene dendrons that act as electroactive surfactants for the capping of CdSe nanocrystals through a ligand exchange process. The number of dendrons per nanocrystal and the nature of surface coordination interactions were studied in detail using UV–vis, FT-IR, AFM, and photoluminescence spectroscopies. These dendron/nanocrystal complexes are very soluble in nonpolar solvents and exhibit photoinduced charge-transfer interactions between the two species. One-layer photovoltaic cells were fabricated that showed initial power conversion efficiencies of 0.29%.

Introduction

Semiconductor nanocrystals or quantum dots and their composites with organic surfactants and polymers are of high interest in nanoscience. Some of the best studied systems include cadmium chalcogenides, whose electronic transitions can be tuned over the whole visible range, and whose synthesis can be carried out with remarkable size control and very high crystallinity. Important advancements include the more affordable and practical “green” routes that use alternative cadmium precursors,^{1,2} derived from more traditional organometallic approaches.^{3,4} Although great commercial promise is expected from semiconducting nanocrystals in various fields and disciplines, their stability and surface chemistry must be continuously explored. Because inorganic nanocrystals are metastable species, it has been shown that the workup and processing are mostly related to the nature and structure of the surface ligands, the interface between the organic and inorganic components, and the photochemical stability of the nanocrystal/ligand complex.^{5,6}

It has been demonstrated by Wang et al. that hydrophilic organic dendron ligands can act as superior stabilizers for both high-quality semiconductor and noble-metal nanocrystals.^{6,7} Steric crowding of the dendron may provide a closely packed but thin ligand shell which may be as efficient as a shell formed by ligands with long and flexible alkyl chains. The steric crowding

of a dendron is ideal for filling the spherical ligand layer because the dendron ligands can naturally pack in a cone shape on the surface of the nanocrystals. It was also proposed that inter- and intramolecular entanglement of the dendrons with relatively flexible branches may further slow the diffusion of small molecules or ions from the bulk solution to the interface between a nanocrystal and its ligands. Recently, our group has reported the synthesis of conjugated thiophene dendrimers whose broad absorbance and thus band gap (ΔE_g) can be tuned by varying the number of thiophene units in the dendrimer molecule.⁸ These molecules are also known to form interesting nanostructures on mica and graphite surfaces due to π – π and van der Waals interactions.⁹

CdSe nanocrystals of different shapes and sizes have also shown great promise as active components of light-emitting diodes^{10–12} and photovoltaic cells.^{13–15} One problem that may limit the efficiency of these devices is aggregation of the nanocrystals in a blend structure with conjugated polymers due to differences in the polarity of the two components. Typically, the hydrophobic surface capping agents (usually consisting of long alkyl chain components) that may hinder charge transfer between the two active species are replaced with a hydrophilic moiety such as pyridine, and the nanocrystals are then dispersed into a conjugated polymer matrix

* To whom correspondence should be addressed. E-mail: radvincula@uh.edu.

(1) Peng, Z. A.; Peng, X. *J. Am. Chem. Soc.* **2001**, *123*, 183.
 (2) Peng, X. *Chem.–Eur. J.* **2002**, *8*, 334.
 (3) Murray, C. B.; Norris, D. J.; Bawendi, M. G. *J. Am. Chem. Soc.* **1993**, *115*, 8706.
 (4) Peng, X. G.; Wickham, J.; Alivisatos, A. P. *J. Am. Chem. Soc.* **1998**, *120*, 5343.
 (5) Aldana, J.; Wang, Y.; Peng, X. *J. Am. Chem. Soc.* **2001**, *123*, 8844.
 (6) Wang, Y. A.; Li, J. J.; Chen, H.; Peng, X. *J. Am. Chem. Soc.* **2002**, *124*, 2293.
 (7) Guo, W.; Li, J. J.; Wang, Y. A.; Peng, X. *J. Am. Chem. Soc.* **2003**, *125*, 3901.

(8) Xia, C.; Fan, X.; Locklin, J.; Advincula, R. C. *Org. Lett.* **2002**, *4*, 2067.

(9) Xia, C.; Fan, X.; Locklin, J.; Advincula, R. C. *J. Am. Chem. Soc.* **2004**, *126*, 8735.

(10) Mattoussi, H.; Radzilowski, L. H.; Dabbousi, B. O.; Thomas, E. L.; Bawendi, M. G.; Rubner, M. F. *J. Appl. Phys.* **1998**, *83*, 7965.

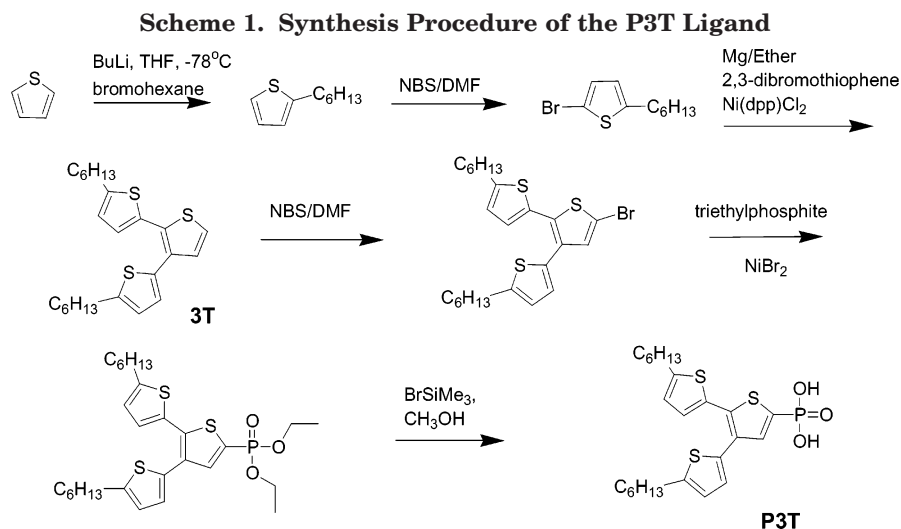
(11) Dabbousi, B. O.; Bawendi, M. G.; Onitsuka, O.; Rubner, M. F. *Appl. Phys. Lett.* **1995**, *66*, 1316.

(12) Gao, M.; Richter, B.; Kirstein, S.; Mohwald, H. *J. Phys. Chem. B* **1998**, *102*, 4096.

(13) Huynh, W. U.; Peng, X.; Alivisatos, A. P. *Adv. Mater.* **1999**, *11*, 923.

(14) Huynh, W. U.; Dittmer, J. J.; Alivisatos, A. P. *Science* **2002**, *295*, 2425.

(15) Sun, B.; Marx, E.; Greenham, N. C. *Nano Lett.* **2003**, *3*, 961.



where phase separation can occur. Recently, Milliron et al. have demonstrated the use of electroactive linear oligothiophene surfactants as mediators of charge transfer between CdSe and organic semiconductors.¹⁶ In their work, they demonstrated the use of phosphonic acid binding groups that have a very high affinity for CdSe nanocrystals. These oligothiophenes underwent energy or electron transfer from the ligand to the nanocrystal depending on the number of thiophene units in the backbone.

In this work, we attempt to combine the stabilizing effect of dendrons and electroactive thiophene moieties to demonstrate stable, conjugated dendron/nanoparticle complexes which undergo efficient hole or electron transfer between the conjugated ligand and the nanocrystal core. The amount of surfactant exchange and the nature of surface binding are studied in detail using various ligand exchange protocols and different branched thiophene capping agents. The electroactive dendrons should provide the nanocrystals with better miscibility as compared to pyridine-capped nanocrystals in a conjugated polymer matrix.

Experimental Section

General Methods. All chemical reagents were purchased from Aldrich Chemical Co. unless otherwise stated. Tetrahydrofuran was distilled over sodium/benzophenone before use. All solvents used for precipitation and separation of nanocrystals and exchange reactions were thoroughly aspirated with N₂ before use.

Characterization. NMR spectra were recorded on a General Electric QE-300 spectrometer at 300 MHz for ¹H NMR and 75 MHz for ¹³C NMR. FT-IR spectra were obtained on a Digilab FTS 7000 equipped with a HgCdTe detector at wavenumbers from 4000 to 600 cm⁻¹. Absorbance spectra were obtained on an HP-8453 diode array spectrometer. Absorbance maxima were kept below 0.5 to stay within the linear region of the Beer–Lambert law in calculating the molar absorptivities for the compounds. Photoluminescence spectra were recorded on a Perkin-Elmer Lambda-45 spectrophotometer. All absorbance values were kept below 0.1 at the excitation wavelength.

AFM Techniques. Samples were prepared by drop-casting a very dilute solution (~1 nM nanocrystals in CHCl₃) onto a

spinning mica substrate at 800 rpm. The mica was freshly cleaved. All solutions were passed through two 0.2 μM hydrophobic fluoropore (PTFE) filters (Millex, Millipore) as they were cast. The surface was then dried under a stream of N₂ before imaging. The samples were examined in ambient conditions with a PicoSPM II (PicoPlus, Molecular Imaging) in the magnetic ac mode (MAC mode). The MAC mode uses a magnetic field to drive a magnetically coated cantilever in the top-down configuration. Type II MAC levers with a spring constant of 2.8 nN/M with about a 10 nm tip radius were used for all scans.

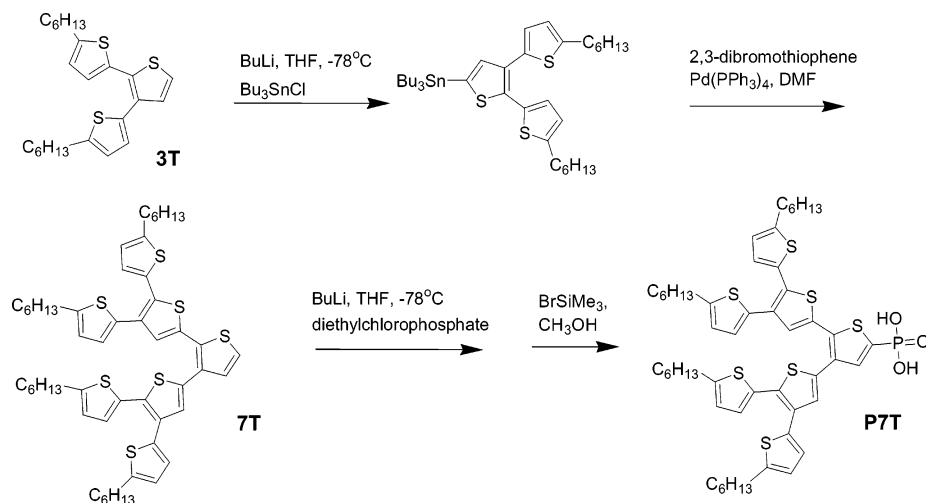
Dendron Synthesis. The synthetic protocol for some of the dendron precursors is shown in Scheme 1. A detailed synthetic procedure for some of these materials has been published previously.⁸

Synthesis of 5,5'-Dihexyl-[2,2';3',2'']terthiophene (3) (3T). The Grignard reagent formed from 7.51 g of 2-bromo-5-hexylthiophene (7.51 g, 30.3 mmol) and magnesium (0.78 g, 32 mmol) was slowly added to a mixture of 2,3-dibromothiophene (3.09 g, 12.76 mmol), Ni(dpp)Cl₂ (7 mg, 0.13 mmol), and 100 mL of ether at 0 °C. After 20 h, the reaction was quenched with dilute HCl, and the organic phase was separated and combined with the ether extraction from the aqueous phase. The solvent was evaporated after drying over magnesium sulfate. The residue was then run through a flash column using hexanes as eluent. A pale yellow viscous liquid was obtained (4.62 g, yield 87%). ¹H NMR (in CDCl₃): δ 7.20 (d, 1H, *J* = 5.3 Hz), 7.11 (d, 2H, *J* = 5.3 Hz), 6.93 (d, 1H, *J* = 3.5 Hz), 6.86 (d, 1H, *J* = 3.5 Hz), 6.67 (d, 1H, *J* = 3.5 Hz), 6.64 (d, 1H, *J* = 3.5 Hz), 2.77 (t, 4H), 1.65 (m, 4H), 1.34 (m, 12H), 0.88 (t, 6H, 6.5 Hz). ¹³C NMR (in CDCl₃): δ 147.53, 146.03, 134.99, 132.30, 132.12, 131.35, 129.62, 127.64, 125.94, 124.15, 124.01, 123.98, 31.59, 31.55, 30.18, 30.12, 28.79, 28.77, 22.68, 22.61, 14.11. Anal. Calcd for C₂₄H₃₂S₃: C, 69.17; H, 7.74; S, 23.09. Found: C, 69.42; H, 7.61; S, 22.98.

Synthesis of 5'-Bromo-5,5'-dihexyl-[2,2';3',2'']terthiophene. In the absence of light, 1.96 g of *N*-bromosuccinimide (NBS; 11.0 mmol) in 15 mL of dimethylformamide (DMF) was added dropwise to a solution of 4.16 g of 3T (10.0 mmol) in 5 mL of DMF at 0 °C. The reaction mixture was stirred overnight and then poured into water. After extraction with hexane, the organic layer was dried over MgSO₄ and concentrated. A pale yellow viscous liquid was obtained by chromatography on silica gel using hexane as eluent (4.32 g, yield 87.1%). ¹H NMR (in CDCl₃): δ 7.08 (s, 1H), 6.90 (d, 1H, *J* = 3.6 Hz), 6.83 (d, 1H, *J* = 3.3 Hz), 6.67 (d, 1H, *J* = 3.6 Hz), 6.63 (d, 1H, *J* = 3.3 Hz), 2.76 (m, 4H), 1.64 (m, 4H), 1.31 (m, 12H), 0.88 (t, 6H, 6.6 Hz). ¹³C NMR (in CDCl₃): δ 148.08, 146.44, 133.54, 132.48, 132.27, 131.85, 130.89, 128.00, 126.21, 124.09, 123.89, 110.646, 31.41, 30.03, 29.94, 28.62, 22.47, 13.98.

(16) Milliron, D. J.; Alivisatos, P.; Pitois, C.; Edder, C.; Frechet, J. M. J. *Adv. Mater.* **2003**, *15*, 58.

Scheme 2. Synthesis Procedure of the P7T Ligand



Synthesis of 5,5''-Dihexyl-[2,2';3',2'']terthiophene-ylphosphonic Acid Diethyl Ester.¹⁷ A mixture of 2.48 g of 5'-bromo-5,5''-dihexyl-[2,2';3',2'']terthiophene (5.0 mmol), 2.5 g of triethyl phosphite, and 0.25 g of NiBr₂ was heated to 135 °C overnight under N₂. The reaction mixture was first cooled to room temperature, and triethyl phosphite was removed by vacuum distillation. The residue was purified by flash column chromatography on silica gel using hexane/dichloromethane/ethyl acetate (5:1:2) as eluent (yellow liquid, 1.67 g, yield 60.4%). ¹H NMR (in CDCl₃): δ 7.61 (d, 1H, *J* = 8.7 Hz), 6.98 (d, 1H, *J* = 3.0 Hz), 6.88 (d, 1H, *J* = 3.0 Hz), 6.68 (d, 1H, *J* = 3.3 Hz), 6.66 (d, 1H, *J* = 3.3 Hz), 4.17 (m, 4H), 2.77 (t, 4H, *J* = 8.0 Hz), 1.64 (p, 4H, *J* = 7.2 Hz), 1.31 (m, 18H), 0.88 (t, 6H, 6.6 Hz). ¹³C NMR (in CDCl₃): δ 148.59, 146.74, 138.94, 138.80, 133.35, 132.69, 132.48, 130.79, 128.12, 126.61, 124.30, 124.04, 62.73, 62.65, 31.43, 31.40, 31.37, 30.02, 29.97, 28.61, 22.46, 16.24, 16.16, 13.97. ³¹P NMR (in CDCl₃): δ 11.72 (s).

Synthesis of 5,5''-Dihexyl-[2,2';3',2'']terthiophene-ylphosphonic Acid.¹⁸ To 1.07 g of 5,5''-dihexyl-[2,2';3',2'']terthiophenylphosphonic acid diethyl ester (1.94 mmol) was added 2.0 g of bromotrimethylsilane dropwise with a needle under N₂. The reaction mixture was stirred for 2 h. Bromotrimethylsilane was removed with a house vacuum, and then 30 mL of methanol was added. The reaction mixture was refluxed for 4 h and concentrated to give a gray solid (0.94 g, yield 97.7%). ¹H NMR (in CDCl₃): δ 7.63 (d, 1H, *J* = 9.6 Hz), 6.92 (d, 1H, *J* = 3.0 Hz), 6.82 (d, 1H, *J* = 3.3 Hz), 6.62 (d, 1H, *J* = 3.0 Hz), 6.56 (d, 1H, *J* = 3.3 Hz), 3.74 (br, 2H), 2.73 (m, 4H), 1.61 (m, 4H), 1.29 (m, 12H), 0.87 (m, 6H). ¹³C NMR (in CDCl₃): δ 148.06, 146.27, 138.99, 138.02, 133.43, 132.59, 132.38, 130.97, 128.21, 126.72, 124.02, 123.79, 31.44, 31.39, 31.34, 30.02, 29.94, 28.69, 22.49, 13.99. ³¹P NMR (in CDCl₃): δ 14.32 (s). FTIR (KBr): 3300–2400 (v, br, OH), 3068 (C–H_{arom}), 2957, 2927, 2871, 2853 (C–H), 1467, 1180 (P=O), 1063 (Ar–P–O), 1014 (P–O–H_{sy}), 998 (P–O–H_{asy}), 920 (Ar–P–O), 859, 802.

Synthesis of Tributyl(5,5''-dihexyl-[2,2';3',2'']terthiophene-5'-yl)stannane (4). BuLi (2.5 M in hexane) (2.43 mL, 6.06 mmol) was added to a solution of (5,5''-dihexyl-[2,2';3',2'']terthiophene (2.3 g, 5.5 mmol) in THF at –78 °C. After 45 min, tributyltin chloride (1.99 g, 6.1 mmol) was added to the mixture. The reaction was allowed to warm to room temperature for 3 h. After normal workup, the product (pale yellow liquid) was used further without other purifications (estimated yield from NMR, 80%). ¹H NMR (in CDCl₃): δ 7.11 (s, 1H), 6.91 (d, 1H, *J* = 3.5 Hz), 6.87 (d, 1H, *J* = 3.5 Hz), 6.66 (d, 2H, *J* = 3.5 Hz), 2.78 (m, 4H), 1.65 (m, 4H), 1.57 (m, 6H), 1.36 (t, 6H, *J* = 7.3 Hz), 1.30 (m, 12H), 1.12 (t, 6H, *J* = 8.3 Hz), 0.92 (m, 15H). ¹³C NMR (in CDCl₃): δ 135.36, 133.05, 132.92,

126.82, 125.78, 124.11, 124.00, 31.63, 31.61, 31.59, 31.56, 30.19, 30.17, 28.96, 28.82, 28.79, 27.30, 22.61, 14.11, 13.70, 10.86.

Synthesis of 2,3-Di(5,5''-dihexyl-[2,2';3',2'']terthiophene-5'-yl)thiophene (5) (7T). A one-neck flask was charged with 3.72 g of 4, 0.425 g of 2,3-dibromothiophene (1.75 mmol), 0.01 g of Pd(PPh₃)₄, and 30 mL of DMF. After three freeze–thaw cycles, the mixture was heated to 100 °C. After 24 h, the mixture was poured into water, extracted with methylene chloride, and washed thoroughly with KF solution to remove tributyltin chloride. The organic layer was then dried over magnesium sulfate, and the solvent evaporated. The residue was purified by flash column chromatography using hexanes/methylene chloride (10:1) as eluent (viscous orange liquid) (1.31 g, yield 82%). ¹H NMR (in CDCl₃): δ 7.28 (d, 1H, *J* = 5.3 Hz), 7.21 (s, 1H), 7.18 (s, 1H), 7.17 (d, 1H, *J* = 5.3 Hz), 6.94 (d, 1H, *J* = 1.7 Hz), 6.93 (d, 1H, *J* = 1.7 Hz), 6.88 (d, 1H, *J* = 3.5 Hz), 6.86 (d, 1H, *J* = 3.5 Hz), 6.51 (m, 4H), 2.79 (t, 8H, *J* = 7.0 Hz), 1.67 (p, 8H, *J* = 7.0 Hz), 1.34 (m, 24H), 0.91 (t, 12H, *J* = 6.4 Hz). ¹³C NMR (in CDCl₃): δ 134.50, 132.94, 132.58, 132.22, 131.95, 131.90, 131.85, 131.69, 131.45, 131.13, 130.47, 129.68, 129.32, 127.59, 127.44, 126.34, 126.15, 124.87, 124.17, 124.14, 124.01, 124.00, 31.58, 31.56, 30.17, 30.13, 28.79, 28.76, 22.60, 22.59, 14.10. Anal. Calcd for C₅₂H₆₄S₇: C, 68.37; H, 7.06; S, 24.57. Found: C, 68.57; H, 7.10; S, 24.28.

Synthesis of 2,3-Di(5,5''-dihexyl-[2,2';3',2'']terthiophene-5'-yl)thiophene-ylphosphonic Acid Diethyl Ester (6). BuLi (2.5 M in hexane) (0.242 mL, 0.55 mmol) was added to a solution of 2,3-di(5,5''-dihexyl-[2,2';3',2'']terthiophene-5'-yl)thiophene (0.5 g, 0.55 mmol) in THF at –78 °C. After 45 min, diethyl chlorophosphate (0.189 g, 1 mmol) was added through an addition funnel. The reaction was allowed to warm to room temperature for 24 h. After extraction with methylene chloride, the organic layer was dried over magnesium sulfate and the solvent removed by evaporation. The residue was purified using hexanes/methylene chloride (8:2) as eluent. ¹H NMR (in CDCl₃): δ 7.68 (d, 1H, *J* = 8.7 Hz), 7.24 (s, 1H), 7.19 (s, 1H), 6.95 (m, 2H), 6.85 (t, 2H, *J* = 3.6 Hz), 6.66 (m, 4H), 4.20 (m, 4H), 2.76 (t, 8H), 1.63 (m, 8H), 1.41–1.25 (m, 30H), 0.88 (t, 12H, *J* = 6.4 Hz).

Synthesis of 2,3-Di(5,5''-dihexyl-[2,2';3',2'']terthiophene-5'-yl)thiophene-ylphosphonic Acid (P7T). Bromotrimethylsilane (0.38 g, 2.48 mmol) was added to a solution of 2,3-di(5,5''-dihexyl-[2,2';3',2'']terthiophene-5'-yl)thiophene-ylphosphonic acid diethyl ester (0.325 g, 0.31 mmol) in THF, and the solution was stirred overnight. The solvent was removed with a rotovap, and bromotrimethylsilane was removed with a house vacuum. Then 30 mL of methanol and 5 mL of THF were added. The reaction mixture was refluxed for 4 h and concentrated to give a dark brown viscous oil (0.29 g, yield 95%). ¹H NMR (in CDCl₃): δ 8.32 (br, 2H), 7.73 (d, 1H, *J* = 9.2 Hz), 7.20 (s, 1H), 7.14 (s, 1H), 6.88 (m, 2H), 6.81

(17) Tavs, P. *Chem. Ber.* **1970**, *103*, 2428.

(18) McKenna, C. E.; Higa, M. T.; Cheung, N. H.; McKenna, M.-C. *Tetrahedron Lett.* **1977**, *2*, 155.

(d, 2H, $J = 3.1$ Hz), 6.60 (m, 4H), 2.73 (m, 8H), 1.62 (m, 8H), 1.29 (m, 24H), 0.88 (t, 6H). ^{13}C NMR (in CDCl_3): δ 147.95, 147.61, 146.51, 146.26, 134.67, 134.21, 134.18, 133.61, 132.49, 132.15, 132.09, 132.04, 131.75, 131.27, 131.08, 130.15, 127.97, 127.76, 126.67, 126.45, 124.31, 124.25, 124.13, 124.09, 31.72, 31.68, 31.63, 30.30, 30.27, 29.85, 28.93, 22.74, 14.23. FT-IR (KBr): 3200–2509 (v, br, OH), 3067 (C–H), 2955, 2928, 2855 (C–H), 1627, 1466 (C=C), 1437 (CH_3), 1374 (C–C), 1184 (P=O), 1053 (Ar–P), 1011 (P–O–H), 927 (Ar–P), 796 (C–H_{def}).

Nanocrystal Synthesis. CdSe nanocrystals were synthesized and purified using a modification of the previously described “green” approach by Peng et al.¹ Briefly, trioctylphosphine oxide (TOPO) (1.15 g, 3.0 mmol), octadecylamine (ODA) (3.18 g, 11.8 mmol), hexylphosphonic acid (0.132 g, 0.8 mmol), and CdO (0.51 g, 0.4 mmol) were added to a Schlenk flask and heated under vacuum at 80 °C. The flask was backfilled with N_2 and heated to 300–320 °C until a colorless solution was obtained. The temperature was lowered to 270 °C, and 2.5 mL of Se (0.2 M in trioctylphosphine (TOP)) was added. The reaction was stopped by removal of the heating mantle when the desired size of the nanocrystals was obtained. After the solution cooled to about 60 °C, 10–20 mL of degassed CHCl_3 was added to the flask, and the solution was centrifuged to remove unreacted precursors. The nanoparticles were then precipitated with degassed methanol, after which centrifugation and decantation were performed to remove any unbound organic material. The process of redispersal and precipitation was repeated several times. The nanocrystals were used immediately for all exchange reactions reported below.

Ligand Exchange. The nanocrystals and dendron surfactants were codissolved in CHCl_3 and allowed to stir for at least 24 h under an inert atmosphere. The product was precipitated in methanol to remove the displaced TOPO and any excess of new surfactant. Redispersion and precipitation were continued in CHCl_3 and methanol until no excess ligand was detected by UV–vis in the wash solution. This was typically 3–6 times depending on the surfactant undergoing exchange. To completely exchange the TOPO ligand for the dendron, it was found necessary to first displace the TOPO with pyridine by stirring in pyridine overnight in a glovebox and precipitating the pyridine-coated nanocrystals in hexane. After washing, the nanocrystals were dispersed in CHCl_3 with an excess of P3T or P7T, after with they were stirred for at least 24 h under an inert atmosphere. The workup procedure was the same as described above.

Device Fabrication. The P7T/nanocrystals were spin-cast onto indium tin oxide (ITO)-coated glass substrates (cleaned by the RCA method)¹⁹ at 1200 rpm for 60 s. The thickness of the layer was ~50–80 nm (as determined by AFM profilometry). Aluminum (100 nm) was evaporated on the active layer at a rate of 0.5–1.0 Å/s. The active area of the device was 0.23 cm^2 . The current–voltage characteristics were measured using a Keithley 236 source measure unit with a Oriel Hg–Xe lamp hooked up to a monochromator. At least 10 devices were tested, and the values given below are an average of all working devices. The incident power (P_{in}) was 0.14 mW/cm^2 . The power conversion efficiency (η_e) was calculated according to the following equation:

$$\eta_e = I_{\text{sc}} V_{\text{oc}} (\text{FF}) / I_{\text{in}}$$

where I_{sc} is the short-circuit current density (mA/cm^2), V_{oc} is the open-circuit voltage, I_{in} is the intensity of irradiating light (mW/cm^2), and FF (fill factor) is defined as

$$\text{FF} = \max\{IV\} / I_{\text{sc}} V_{\text{oc}}$$

Results and Discussion

Figure 1 shows the FTIR absorbance spectra of TOPO, P3T, P7T, and CdSe nanocrystals at various intervals in the synthesis and exchange process. The P=O stretch

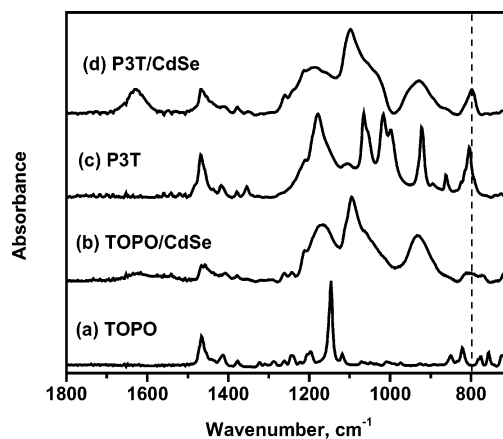


Figure 1. FT-IR spectra of TOPO, P3T, and CdSe nanocrystals before and after exchange with the dendrons in the P=O stretching region.

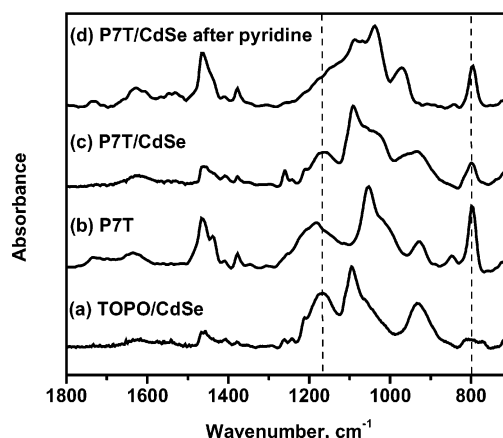


Figure 2. FT-IR spectra in the P=O stretching region of TOPO-capped CdSe, P7T ligand, and P7T-capped CdSe nanocrystals after exchange.

of the TOPO ligand at 1149 cm^{-1} is broadened into three major bands centered at 1166, 1095, and 929 cm^{-1} . The splitting with a shift to lower energy of the major band (1095 cm^{-1}) could imply some multidentate coordination through occupation of bridging positions over the Cd sites.^{20,21} It is also possible that TOP/Se, hexylphosphonic acid from the Cd precursor, or an impurity in the TOPO (technical grade, 90%) such as octylphosphonic or -phosphinic acid is contributing to the nanoparticle surface as has been determined by other groups.²² It is worth noting that the major capping agent with CdSe nanorods was found to be phosphonic acids by dissolving the nanoparticles and analyzing the ligands with NMR.²³ The rest of the peaks in the spectrum of TOPO and the TOPO-capped nanocrystals do not change with respect to position, shape, or intensity (not shown), which implies that the other groups are not in contact with the surface of the nanocrystal or tightly packed on the nanocrystal surface.

The spectrum of P3T is shown in Figure 1c, where the P=O (1180 cm^{-1}), Ar–P–O (1065 cm^{-1}), P–O–H_(as,s)

(20) Katari, J. E. B.; Colvin, V. L.; Alivisatos, A. P. *J. Phys. Chem.* **1994**, *98*, 4109.

(21) Eilon, M. J.; Mokari, T.; Banin, U. *J. Phys. Chem. B* **2001**, *105*, 12726.

(22) Kuno, M.; Lee, J. K.; Dabbousi, B. O.; Mikulec, F. V.; Bawendi, M. G. *J. Chem. Phys.* **1997**, *106*, 9869.

(23) Peng, Z. A.; Peng, X. *J. Am. Chem. Soc.* **2002**, *124*, 3343.

(19) Kern, W. *Semicond. Int.* **1984**, 94.

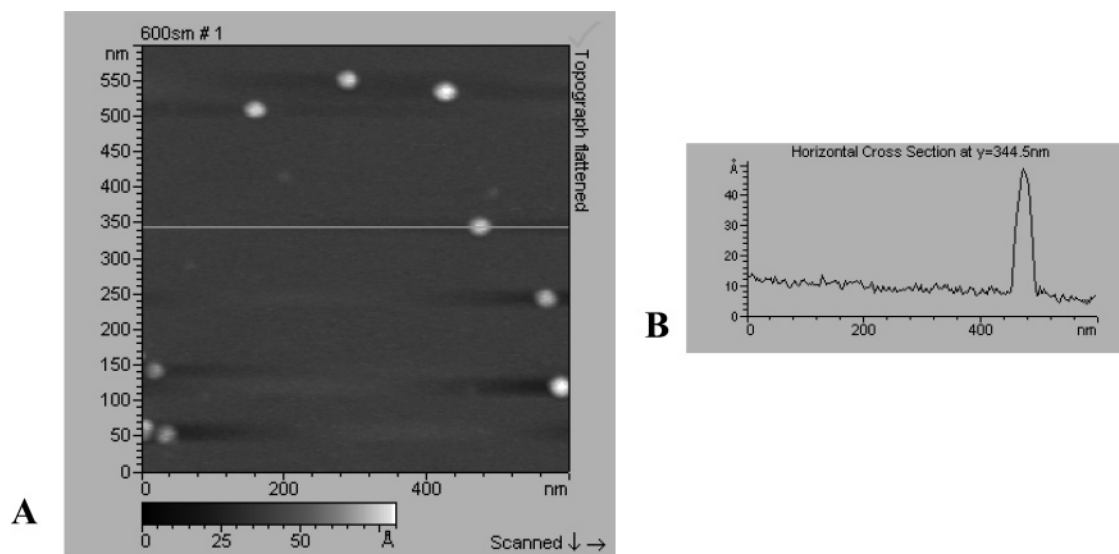


Figure 3. (A) MAC mode AFM image and (B) cross section analysis of P7T/CdSe nanocrystals (~ 1 nm) drop-cast onto a mica substrate spinning at 800 rpm.

(1016, 997 cm^{-1}), and Ar–P–O (922 cm^{-1}) peaks are tentatively assigned.^{24–26} The C–H out of plane vibration of the substituted thiophene ring is assigned to 804 cm^{-1} . Figure 1d shows the spectrum of the P3T/CdSe complex after exchange from TOPO-capped nanocrystals. The peaks are broadened significantly and resemble a combination of P3T and TOPO, indicating an inefficient exchange. This was also evident from the NMR spectrum, where a significant amount of TOPO was detected in the nanocrystal complex.

The spectrum of P7T is shown in Figure 2b, where the P=O (1183 cm^{-1}), Ar–P–O (1053 cm^{-1}), P–O–H (1011 cm^{-1}), and Ar–P–O (929 cm^{-1}) peaks are assigned. The peaks are broadened significantly probably due to intermolecular hydrogen bonding between molecules. The C–H out of plane vibration of the substituted thiophene ring is assigned to 796 cm^{-1} .^{27,28} Figure 2c,d shows the spectra of the P7T/CdSe complex after exchange directly from TOPO/CdSe and pyridine-capped nanocrystals. The peak at 796 cm^{-1} is evident of the binding of P7T to the nanocrystal surface. The intensity of the P=O stretching vibration at 1183 cm^{-1} has decreased due to Lewis acid coordination to Cd atoms. The P–OH band remains, indicating the absence of condensation, and is shifted slightly to higher wavenumbers.

Figure 3 shows the AFM image of single P7T/CdSe nanocrystals drop-cast on mica. The particles were found to be nearly monodispersed, with an average height of 3.84 nm. The height profile of 35 particles was sampled.

The top part of Figure 4 shows the absorbance and emission spectra for P3T and the TOPO-capped CdSe nanocrystals used for the ligand exchange. P3T has an

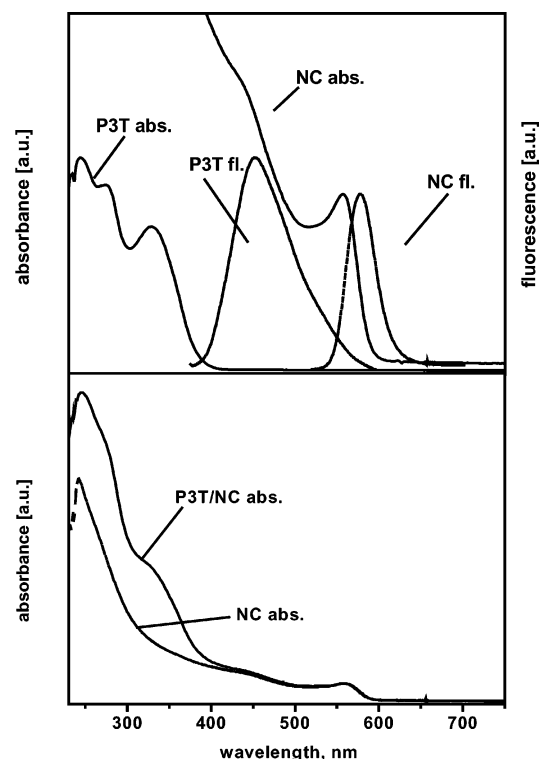


Figure 4. Absorption and fluorescence spectra of P3T and NC (top) in CHCl_3 . The bottom graph is of the P3T/NC complex. The fluorescence for both P3T and NC is completely quenched in the complex. Deconvolution yields about 53 P3T molecules per NC. For more details, see the text.

absorption maximum at 249 nm accompanied by two shoulders at 270 and 330 nm. The emission has a significant Stokes shift with a maximum at 452 nm. P3T has a quantum yield of $\sim 6\%$ in CHCl_3 with respect to diphenylanthracene in cyclohexane. The specific absorption coefficient was $\epsilon = 11400 \text{ L mol}^{-1} \text{ cm}^{-1}$ at 330 nm as calculated from the Beer–Lambert law. The nanocrystals shown in the figure were synthesized by a method similar to that of Peng et al. using CdO.^{1,2} The absorbance maximum at the first excitonic peak was 556 nm, and the photoluminescence maximum was 576 nm. The quantum yield of the CdSe nanocrystals was $\sim 5\%$

(24) Corbridge, D. E. C. Phosphorus Compounds. *Topics in Phosphorous Chemistry*; Wiley & Sons: New York, 1969; Vol. 6.

(25) Artzi, R.; Daube, S. S.; Cohen, H.; Naaman, R. *Langmuir* **2003**, *19*, 7392.

(26) Chalmers, J. M.; Griffiths, P. R. *Handbook of Vibrational Spectroscopy*; Wiley: Chichester, U.K., 2002.

(27) Hotta, S.; Rughooputh, S. D. D. V.; Heeger, A. J.; Wudl, F. *Macromolecules* **1987**, *20*, 212.

(28) Socrates, G. *Infrared Characteristic Group Frequencies*; Wiley: Chichester, U.K., 1980.

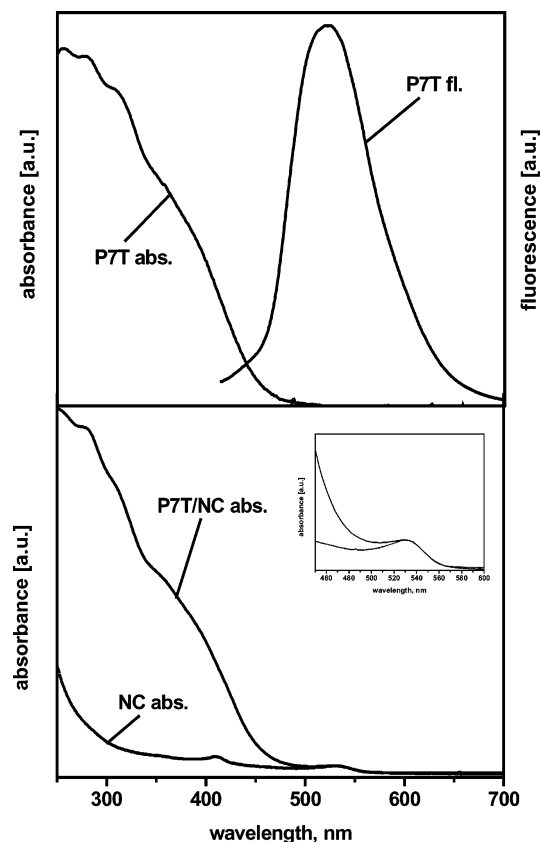


Figure 5. Absorption and fluorescence spectra of P7T in CHCl_3 . The bottom graph is of the P7T/NC complex. The fluorescence for both P7T and NC is completely quenched in the complex. Deconvolution yields about 34 P7T molecules per NC. For more details, see the text.

when TOPO was used exclusively in the reaction and slightly higher (8–12%) when a mixture of ODA/TOPO was used. Size and extinction coefficients at the first excitonic absorption peak for the nanocrystals were calculated using the empirical fitting functions published previously.²⁹ The nanoparticles shown in Figure 3 had a diameter of 3.17 nm and $\epsilon = 124320 \text{ L mol}^{-1} \text{ cm}^{-1}$ at 556 nm.

The bottom part of Figure 4 shows the spectrum of the nanocrystal/ligand complex after exchange. The absorbance resembles a superposition of the two species with no other apparent peaks or features present. Also shown is the nanocrystal absorbance before exchange to show that no change in the first excitonic absorption has occurred. Care was taken to make sure that no unbound P3T remained in the measurements, as several precipitation and washing steps were taken until no unbound P3T could be detected in the washing solution. The figure also shows that the fluorescence in the two species is completely quenched. The spectrum can be deconvoluted using the molar absorption coefficients of the two species and subtracting out the nanoparticle absorbance to reveal an average of 53 P3T molecules per nanocrystal (for a 3.17 nm diameter).

The top part of Figure 5 shows the absorbance and emission spectra of P7T. The absorbance is broad with a maximum at 255 nm, several features at 280, 309, and 368 nm, and a tail ending around 470 nm. The

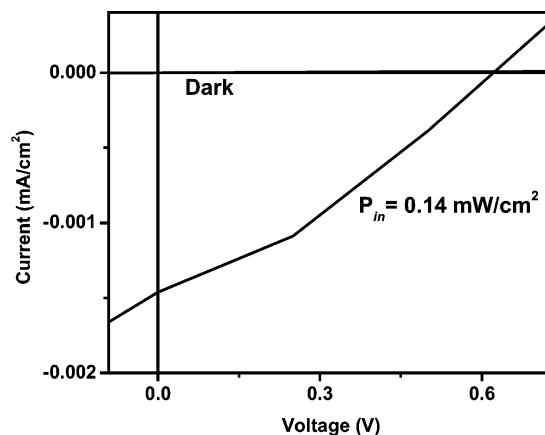


Figure 6. Current density vs voltage for a P7T/CdSe device in the dark and under 0.14 mW/cm^2 illumination.

broadness is due to the different conjugation pathways between the thiophene rings. The emission spectrum has a maximum at 521 nm, and the quantum yield is 25%. The specific absorption coefficient was $23300 \text{ L mol}^{-1} \text{ cm}^{-1}$ at 280 nm.

The bottom part of Figure 5 shows the absorbance and photoluminescence of the P7T/nanocrystal complex. The inset shows the absorbance of the nanocrystals before and after exchange ($\lambda_{\text{max}} = 536 \text{ nm}$, diameter 2.79 nm). After deconvolution, it was determined that an average of 30 P7T dendrons coated each nanocrystal. As with the P3T, the photoluminescence of both the nanocrystals and the P7T is completely quenched. To ensure that the phosphonic acid binding moiety was completely passivating the surface and not just inducing surface defects that could quench the fluorescence, we tried both phenylphosphonic acid (as also stated by Milliron et al.)¹³ and a thiophene derivative with a phosphonic acid headgroup under the same exchange protocols and found an enhancement in the fluorescence of the nanocrystals after the TOPO exchange. The quenching can be the result of electron transfer between the ligand and nanocrystals.

To test the effect of nonradiative energy transfer, i.e., direct photocurrent conversion, a simple photovoltaic device was prepared. The dendron/nanocrystal complexes should undergo photoexcited charge transfer between the two species. Figure 6 shows the current–voltage curves of one-layer devices made using the P7T/CdSe nanocrystals by spin-coating on ITO. The average results of at least 10 different working devices showed that $V_{\text{oc}} = 0.6 \text{ V}$, $I_{\text{sc}} = 1.56 \times 10^{-6} \text{ A/cm}^2$, $\text{FF} = 0.3$, $P_{\text{in}} = 0.14 \text{ mW/cm}^2$, and the power conversion efficiency $\eta_e = 0.29\%$. It is expected that electron transport in this device is limited by the small size of the nanocrystals. In principle, the efficiency can be further optimized by increasing the size and changing the shape of the nanocrystals.

Conclusions

In this work, we have demonstrated the use of conjugated oligothiophene dendrons as successful capping agents for CdSe nanocrystals. The size of the dendron and competition with intermediate ligands, e.g., pyridine, allow a stepwise ligand exchange procedure. The P7T-capped nanocrystals have excellent solubility

(29) Yu, W. W.; Qu, L.; Guo, W.; Peng, X. *Chem. Mater.* **2003**, *15*, 2854.

in a wide variety of nonpolar solvents, which can provide greater miscibility in a conjugated polymer matrix that is necessary for improved hole transport in thin film semiconductor devices. The dendron/nanocrystal complexes undergo photoexcited charge transfer between the two species, which should prove ideal for certain devices such as bulk-heterojunction photovoltaic cells in which the separation of charge upon photoexcitation is necessary for high efficiency. Thus, one-layer photovoltaic devices have been fabricated which showed a power conversion efficiency of 0.29%. It is assumed that this value can be greatly improved by increasing the size and shape of the nanocrystals through improved

electron transport. Extensive research involving the incorporation of larger generations of dendrons that have a broader absorbance with CdSe nanocrystals and blending with regioregular polythiophenes is under way.

Acknowledgment. We gratefully acknowledge support from various funding agencies that made this work possible: The NSF (Grants DMR-99-082010 and CHE-03-04807), Robert A. Welch Foundation (Grant E-1551), NSF-CTS (Grant 03-30127). Technical support from Molecular Imaging and Digilab is also greatly acknowledged.

CM048961Q